IJCSE International Journal of Computer Sciences and Engineering Open Access
Research Paper Vol.-6, Issue-12, Dec 2018 E-ISSN: 2347-2693

All-Optical Linear Binary Code Generator Using Optical Nonlinear Material Based Devices

Ashis Kumar Mandal

Department of Physics, Chakur Haris Seminary High School, West Bengal, India

*Corresponding Author: ashiskumarmandal7@gmail.com

Available online at: www.ijcseonline.org

Accepted: 08/Dec/2018, Published: 31/Dec/2018

***Abstract*:** The transmission of information occurs simultaneously over the same available channel bandwidth in Code Division Multiple Access (CDMA) technique. The spread spectrum (SS) technique is employed in CDMA systems for transmission of information by employing spreading codes. A unique spreading code, acts as a signature code, is assigned for each individual user. The signal occupies a bandwidth much larger than the minimum necessary to send the information in SS modulation technique. A synchronized reception with the code at the receiver is applied for dispreading the information before data recovery. From a long-term, Walsh-Hadamard codes have been employed as spread spectrum codes in CDMA communications due to their ease of generation than the efficiency of these codes. Walsh-Hadamard codes are absolutely orthogonal linear binary codes which have so many favorite applications in synchronous multicarrier communications though they perform poorly for asynchronous multi-user communications. Now, the optical application of these Walsh-Hadamard codes is important for optical CDMA. In these designs nonlinear optical property is exploited for capable of controlling multi-valued signals. To this purpose, it is proposed with exploiting the polarization properties of light an all-optical design of Walsh-Hadamard codes generator in this paper.

***Keywords*:** Optical nonlinear material, Optical switches, Polarization converter, Polarization converter mask, Walsh-Hadamard code.

I. INTRODUCTION

CDMA technique has been considered as important multiple access schemes in the second-generation (2G), third-generation (3G) and also future broadband wireless systems. CDMA has attractive features, like anti-jam resistance, low probability of interception, resistance to multipath fading, and capability of random access over conventional access techniques such as time division multiple access (TDMA) and frequency division multiple access (FDMA). Orthogonal codes are widely used for uplink and downlink transmissions of cellular DS-CDMA systems and WCDMA/UMTS. Many of the spreading codes are used in wireless communication today, they are fixed power codes and are restricted in their power levels, the availability of the code family sizes. In our traditional cellular networks, binary Walsh-Hadamard codes are employed as CDMA spreading codes. Walsh-Hadamard codes are applied for synchronous communications. Longer distances in our traditional cellular networks demand higher processing gain, thus requiring longer spreading codes in CDMA. Popularity of these codes comes from the ease of their implementation utilizing standard kernels. Optical-Code Division Multiple Access (O-CDMA) is a promising technology for high-performance local area networks with flexible assignment of network capacity. Code division multiplexing (CDM) gives an alternative to the traditional methods of time-division multiplexing (TDM) and frequency division multiplexing (FDM). CDMA does not need the bandwidth allocation of FDMA, or the time synchronization needed in TDMA. But, users of a common channel are allowed to access simultaneous assignment of mutually (near) orthogonal spreading codes. These methods for generating spreading codes with required auto correlation and cross correlation properties for CDMA have been improved such as Gold, Kasami codes, Walsh-Hadamard codes etc. Walsh codes are practiced broadly in CDMA/multi carrier CDMA (MC-CDMA) because of its orthogonal character and good auto-correlation property [1-6].

In present, this design and application of Walsh-Hadamard codes is not limited to the realm of electronics only but also extended to optics also. All-optical realization of this code emerges to overcome the electronic bottlenecks and to exploit fully the advantages of fiber optic communication without essence of optical-electrical-optical (OEO) conversions. The techniques of computing by using light, i.e. photon which is being the ultimate unit of information with unmatched speed and with data package in a mass zero signals, may provide a way out of the limitations of computational speed and inherent complexity in electronics

systems [7]. Theta modulation, optical shadow casting technique, symbolic substitution and semiconductor amplifier based Interferometric switches etc. are reported in several literatures for application of binary logic operations [8-10].

In recent years for optical logic and information processing, optical multiple valued logic functions takes great attraction of research community due to fact that it needs less physical space than binary data [11]. Liu et al has presented bi-stable laser diode for optical demonstration of multiple valued logic circuits [12]. Eichmann et al has explained binary coded trinary arithmetic and logic operation [13]. Intensity of light signal is indicate the logic states in few cases to realize the Boolean logic operations that want well defined specific intensity of light for every cases. The intensity of signal may be altered due to many reasons and these difficulties can be prevented in polarization based encoding/decoding technique [11].

We present an all-optical technique of Walsh-Hadamard code generation in this paper using terahertz optical asymmetric demultiplexer (TOAD) and optical nonlinear material based optical switches [14-18]. For this optical implementation the set of logic states are chosen as shown below:

0 = vertically polarized light (↕), 1 = horizontally polarized light (•); -1 = plane polarized light at 45^0 (⤢). The proposed paper is arranged as follows: The working principle and tree architecture of TOAD are reported in Section II. Section III describes briefly the optical components (using optical nonlinear material based switches) used with their functions and Section IV presents Walsh code generation using optical nonlinear material based switches. Section V shows mathematical simulation results and finally concluding remarks are made in Section VI.

II. TOAD and its tree architecture

A. Working principle of TOAD based optical switch

In recent age of information, TOAD has taken an important role in optical communication and information processing [19-25]. Sokoloff et al. [18] reported a TOAD capable of demultiplexing data at 50 Gb/s. TOAD exploits the strong, slow optical nonlinearities present in semiconductor and it is characterized with control and signal pulses using polarization or wavelength. It needs less than 1 pJ switching energy. The same authors group has also reported that by reducing the SOA length to 100 μm and increasing its dc bias current, its propagation delay can be reduce to1ps without impacting its performance as a nonlinear element. Then TOAD can perform demultiplexing at Tb/s [22].

The TOAD consists of a loop mirror with an additional intraloop 2×2 (ideally 50:50) coupler and this loop contains a control pulse (CP) and a nonlinear element (NLE) that is offset from the loop's midpoint by a distance Δx as shown in Fig. 1.

A signal with field $E_{in}(t)$ at angular frequency ω is split in coupler. It travels in clockwise (cw) and counter clockwise (ccw) direction through the loop. The electrical field at port-1 and port-2 can be expressed as follows.

$$\underline{E}_{out,1}(t) = \underline{E}_{in}(t-t_d)\cdot e^{-j\omega t_d}\cdot\left[d^2\cdot\underline{g}_{cw}(t-t_d) - k^2\cdot\underline{g}_{ccw}(t-t_d)\right] \quad (1)$$

$$\underline{E}_{out,2}(t) = jdk\underline{E}_{in}(t-t_d)\cdot e^{-j\omega t_d}\cdot\left[\underline{g}_{cw}(t-t_d) + \underline{g}_{ccw}(t-t_d)\right] \quad (2)$$

Where t_d is pulse round trip time within the loop as shown in the fig 1. Coupling ratios *k* and *d* indicate the cross and through coupling, respectively. The cw signal is amplified by the complex field gain. $\underline{g}_{cw}(t)$. And ccw is also amplified by $\underline{g}_{ccw}(t)$.

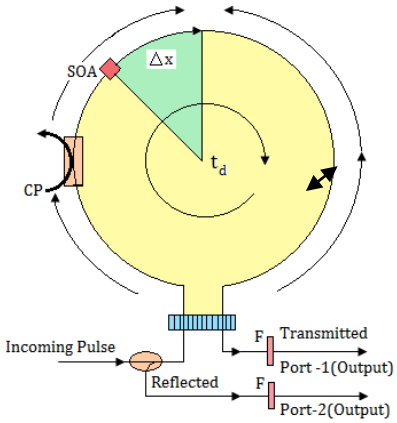

Fig. 1: TOAD-based optical switch

The output power at port-1 can be expressed as,

$$P_{out,1}(t) = \frac{P_{in}(t-t_d)}{4}\cdot\left\{G_{cw}(t)+G_{ccw}(t)-2\sqrt{G_{cw}(t)\cdot G_{ccw}(t)}\cdot\cos(\Delta\varphi)\right\}$$
$$= \frac{P_{in}(t-t_d)}{4}\cdot SW(t)$$

(3) Where, This $SW(t)$ is the transfer function. The phase difference between cw and ccw pulse is defined by $\Delta\varphi = (\varphi_{cw} - \varphi_{ccw})$. The symbols $G_{cw}(t), G_{ccw}(t)$ indicate the respective power gains. Power gain is related with the field gain as $G = g^2$ and $\Delta\varphi = -\frac{\alpha}{2}\cdot\ln\left(\frac{G_{cw}}{G_{ccw}}\right)$.

Now we will calculate the power at port-2

$$P_{out,2}(t) = \frac{1}{2}\underline{E}_{out,2}(t)\cdot\underline{E}^*_{out,2}(t)$$

$$= d^2k^2\cdot P_{in}(t-t_d)\cdot G_{cw}\cdot\left\{1+\frac{G_{ccw}}{G_{cw}}+2\cdot\sqrt{\frac{G_{ccw}}{G_{cw}}}\cdot\cos[\Delta\varphi]\right\}$$

$$= d^2k^2 \cdot P_{in}(t-t_d) \cdot \left\{ G_{cw} + G_{ccw} + 2 \cdot \sqrt{G_{ccw} \cdot G_{cw}} \cdot \cos[\Delta\varphi] \right\}$$

(4)

; For ideal 50:50 coupler $d^2 = k^2 = 1/2$. When control signal is absent, data signal i.e., incoming signal enters the fiber loop and pass through the SOA at different times as they counter-propagate around the loop. They experience the same unsaturated amplifier gain G_0 and recombine at the input coupler i.e. $G_{ccw} = G_{cw}$. This leads to $\Delta\varphi = 0$. So expression for $P_{out,1}(t) = 0$, and $P_{out,2}(t) = G_0 \cdot P_{in}$. It shows that data is reflected back toward the source. When a control pulse is injected into the loop, it saturates the SOA and changes its index of refraction. Therefore the two counter-propagated data signals will experience a differential gain saturation profiles i.e. $G_{ccw} \neq G_{cw}$. When they recombine at the input coupler, the data will exit from the output port-1. Now the mathematical forms of two output powers can be expressed as, $P_{out,1}(t) = \frac{P_{in}(t-t_d)}{4} \cdot SW(t)$ and $P_{out,2}(t) \approx 0$. A polarization or wavelength filter may be used at the output to reject the control and pass the input pulse. The schematic block diagram is shown in Fig. 2 and the truth table of the operation is given in Table-1.

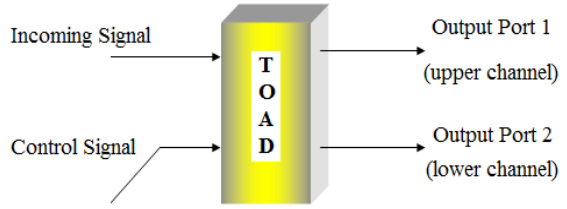

Fig. 2: Schematic diagram of TOAD-based optical switch

Table-1: Truth table of TOAD based optical switch as shown in Fig. 3

Incoming Signal	Control Signal	Output Port-1
0	0	0
0	1	0
1	0	0
1	1	1

(B) Tree Architecture of TOADs: System description of demultiplexer

Tree Architecture or demultiplexer operation requires three TOAD switches, one in first stage and two in the second stage as shown in Fig.3 (b). Final outputs of two TOAD switches in second stage are fed to spectrum analyzers and represent terminals (output ports) T1 through T4. When A=1 and B=1, according to the switching principle discussed earlier the light reaches T_1 (output port-1).In this case, no light is present at other terminals T_2, T_3 and T_4 [25]. The positive spectrum is obtained only at T_1. When A=1 and B=0, light is only present in T_2 (output port-2) thus positive spectrum peak is obtained only at this terminal.

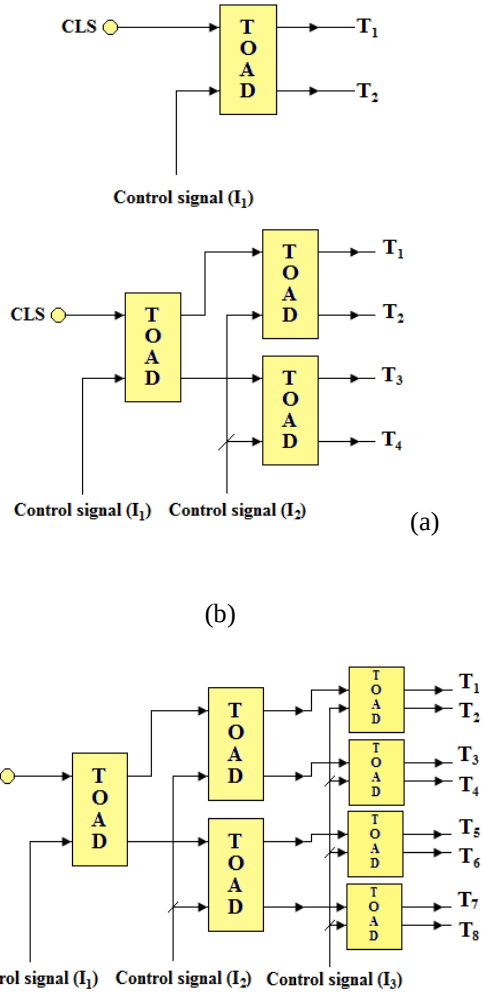

Fig. 3 Tree architecture using TOADs

For the case A=0 and B=1, T_3 (output port-3) is in the one state and others are in zero state. When both control signals are 0, the light is obtained at T_4 (output port-4). Architecture or demultiplexer operation of fig 3 (b) satisfies truth table-3. The operation of tree architecture or demultiplexer of fig 3 (c) is similar with fig 3(b) as described above and satisfies truth table-4. Architecture or demultiplexer operation of fig 3 (a) is similar with fig 2 as described in working principle of TOAD above and satisfies truth table-2.

Table-2: Truth table of TOAD based optical tree architecture of fig. 3(a)

Input A or B			Output
I_1	I_2	I_3	
1	1	1	T_1
1	1	0	T_2
1	1	1	T_3
1	1	0	T_4
1	0	1	T_5
1	0	0	T_6
1	0	1	T_7
1	0	0	T_8
0	1	1	T_9
0	1	0	T_{10}
0	1	1	T_{11}
0	1	0	T_{12}
0	0	1	T_{13}
0	0	0	T_{14}
0	0	1	T_{15}
0	0	0	T_{16}

Table-3: Truth table of TOAD based optical tree architecture of fig. 3(b)

Input A or B	Output
I_1	
1	T_1
0	T_2

Table-4: Truth table of TOAD based optical tree architecture of fig. 3(c)

Input A or B		Output
I_1	I_2	
1	1	T_1
1	0	T_2
0	1	T_3
0	0	T_4

III. Functions of Optical Components and Designing of PCM and PC

The input light is allowed to fall on an input block (IB) after expanding it by Beam Expander (BE). The IB is constructed only for matrix form input without any layers of polarizer isolator mask (PI mask) or polarization converter mask (PCM). The propagation of light signal through IB is as follow that first input light is incident on IB after that it falls on optical nonlinear material (OPNLM) and then emerging signal beam comes out through OPNLM based matrix block as an output light signal.

A. PCM (type-1) design and its function

The PCM (type-1) matrix is also shown in the figure 5 consisting different types of polarization converter, placed in (2x2) matrix form. Jones matrix representation is used for calculation of different types of polarization converter which is needed here. Jones vector which represents three logical states of three types of polarized light can be written as follows.

E_1 = Jones vector of linearly polarized light with horizontal orientation (⬮) = $\begin{bmatrix}1\\0\end{bmatrix}$

E_0= Jones vector of linearly polarized light with vertical orientation (↕) = $\begin{bmatrix}0\\1\end{bmatrix}$

E_{-1}= Jones vector of linearly polarized light at 45^0 (⬈⬊) = $\frac{1}{\sqrt{2}}\begin{bmatrix}1\\1\end{bmatrix}$

Polarization converter (PC) of type-1 (PC-1)

The polarization converter of type-1 is formed by half wave plate ($\lambda/2$) and then Jones matrix for the Half-wave plate is

$$J_H = \begin{bmatrix}\cos(2\rho) & \sin(2\rho)\\ \sin(2\rho) & -\cos(2\rho)\end{bmatrix} \quad (5)$$

Here ρ is azimuth angle of the optical axis, if $\rho=\pi/4$, from the equation (1) we get the Jones matrix $J_H=\begin{bmatrix}0 & 1\\1 & 0\end{bmatrix}$

When 2 $\rho=\pi/4$ then from equation (1) we obtain the Jones matrix $J_H=\frac{1}{\sqrt{2}}\begin{bmatrix}1 & 1\\1 & -1\end{bmatrix}$. Hence, $J_H.E_1 = \frac{1}{\sqrt{2}}\begin{bmatrix}1\\1\end{bmatrix}$ (6)

i.e., optic axis of PC-1 is set $22(1/2)^0$ with (+x)-axis, so that horizontally polarized light (⬮) is converted to plane polarized light at 45^0 (⬈⬊). Only a specific type of polarized light passes through PI mask otherwise PI mask blocks other types of polarized light and PCMs convert the type of polarization of input light signals [26].

B. Mathematical model of OPNLM based switch

Let the signal beam is propagating along Z-axis and the three incident monochromatic waves are [27]

$$E_1(\omega) = a_1A_1(r)e^{-i(\omega t-k_1 r)} \quad (7)$$

$$E_2(\omega) = a_2A_2(r)e^{-i(\omega t-k_2 r)} \quad (8)$$

$$E_3(\omega) = a_3A_3(r)e^{-i(\omega t-k_3 r)} \quad (9)$$

Where, a_1, a_2 and a_3 are the unit vectors along the light polarization direction of the forward beam (or signal beam), backward beam (or signal beam) and the probe beam respectively. K_1 and K_2 are the wave vectors of the two pump waves (or signal beams), k_3 is the absolute value of the wave vector of the probe beam, A_1 and A_2 are the real amplitude functions of the two plane pump waves and A_3 is the complex amplitude function of the signal wave and ω is the frequency of the pump beams (or signal beams) and the probe beam. According to the principle of FWM a fourth coherent wave will be generated through the third order nonlinear polarization response of the medium. The generated wave and its corresponding nonlinear electric polarization of fourth coherent wave will be

$$P_4^{(3)}(\omega) = \varepsilon_0 \chi_e^{(3)}(\omega, \omega, -\omega)\, a_1\, a_2\, a_3\, A_1\, A_2\, A_3^* e^{-i(\omega t + k_3 z)} \quad (10)$$

$$E_4(\omega) = a_4 A_4(z) e^{-i(\omega t + k_3 z)} \quad (11)$$

As it is assumed that the three incident wave are linearly polarized along the same direction (here Z-axis) and the medium is isotropic, so E_4 also will polarized along the same direction. Thus we may neglect the vector property of the fields. So the third order polarization fields for E_3 and E_4 can be written as

$$P_3^{(3)}(\omega) = \varepsilon_0 \chi_e^{(3)} A_1 A_2 A_4^* e^{-i(\omega t - k_3 z)} \quad (12)$$

$$P_4^{(3)}(\omega) = \varepsilon_0 \chi_e^{(3)} A_1 A_2 A_3^* e^{-i(\omega t + k_3 z)} \quad (13)$$

Here, $\chi_e^{(3)}$ is the effective third-order nonlinear susceptibility of the medium.

Substituting Eqs.(12) and (13) in the general nonlinear coupled wave equation and assuming that the depletion of both pump waves (or signal beams) within a short interaction length is negligible, the equations for amplitude variation along X-axis for E_3 and E_4 can be written as

$$\frac{\partial A_3^*(z)}{\partial z} = i \gamma^* A_4(z) \quad (14)$$

$$\frac{\partial A_4(z)}{\partial (z)} = i \gamma A_3^*(z) \quad (15)$$

Where, γ complex coupling co-efficient between the pump beams (or signal beams)

$$= \frac{k_3(\omega)}{2\varepsilon_r(\omega)} \chi_e^{(3)} A_1 A_2 = \frac{\omega}{2 c n_0(\omega)} \chi_e^{(3)} A_1 A_2 \quad (16)$$

Here ε_r and n_0 are the linear dielectric constant and refractive index of the nonlinear medium respectively. Considering A_1, A_2 and γ as constant the solutions of (14) and (15) can be expressed as [28]

$$A_3(z) = \frac{\cos\{|\gamma|(z-l)\}}{\cos(|\gamma| l)} A_3(0) - i \frac{|\gamma|}{\gamma^*} \frac{\sin(|\gamma| z)}{\cos(|\gamma| l)} A_4^*(l) \quad (17)$$

$$A_4(z) = \frac{\cos(|\gamma| z)}{\cos(|\gamma| l)} A_4(l) + i \frac{\gamma}{|\gamma|} \frac{\sin\{|\gamma|(z-l)\}}{\cos(|\gamma| l)} A_3^*(0) \quad (18)$$

Here $A_3(0)$ is the amplitude of the probe beam on the incident surface (z=0) of the nonlinear medium. Considering the boundary $A_3(z) = 0$ at $z = l$ i.e. $A_4(l) = 0$ and hence $A_4^*(l) = 0$ also the final solutions can be written as

$$A_3(l) = \frac{A_3(0)}{\cos(|\gamma| l)}; \quad \text{at } z = l \quad (19)$$

And

$$A_4(0) = -i \frac{\gamma}{|\gamma|} \tan(|\gamma| l) A_3^*(0) \quad (20)$$

Hence Eq. (20) implies that near the incident surface of the nonlinear medium $A_4(0)$ is proportional to $A_3^*(0)$. Again from Eq. (11) we know the wave E_4 is counter propagating to the wave E_3. So we may conclude that E_4 and E_3 are phase conjugated to each other and the system plays the role of a phase conjugate reflector.

Now the Nonlinear intensity reflectivity (R) which is the intensity or energy ratio between the backward phase conjugate beam and the incident probe beam can be obtained from Eq. (20) as

$$R = \frac{I_4}{I_3} = \frac{|A_4(0)|^2}{|A_3(0)|^2} = \tan^2(|\gamma| l) \quad (21)$$

If $(\pi/4) < |\gamma| l < (3\pi/4)$ then R>1, which implies an amplification effect of the backward wave E_4. Again Eq. (19) shows that $A_3(l) > A_3(0)$ i.e. the signal wave E_3 will be always amplified through the nonlinear medium.

$\gamma l << \pi/4$, $R = \gamma^2 l^2$.

So from Eqs.(16) and (21) we can write

$$R = \frac{I_4}{I_3} = \frac{\omega^2}{4 c^2 n_0^2(\omega)} |\chi_e^{(3)}|^2 I_1 I_2 l^2 \quad (22)$$

I_1 and I_2 are intensities of the two pump waves and l is the effective interaction length of the nonlinear medium. So relation (22, 16) shows that the output conjugate beam will come out only when the two pump (or signal) and a probe beams are present, which satisfies the switching mechanism of OPNLM.

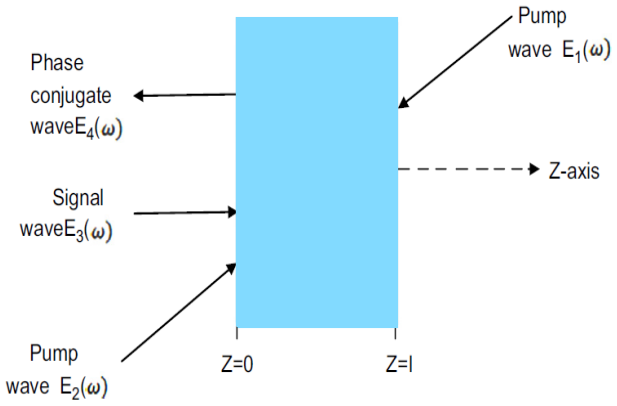

Fig 4(a) Working principle of OPNLM based switch

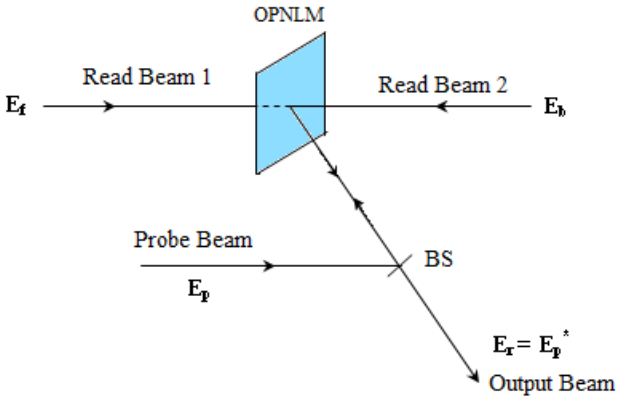

Fig 4(b) Working principle of an OPNLM based switching system (BS is non polarizing beam splitter)

C. OPNLM based (2x2), (4x4) and (8x8) matrixes and their function

The OPNLM matrix that consists of OPNLM based switch and this switching system exploits optical phase conjugation mechanism that has already been explained for its usefulness in binary logic and information processing. Here, for this optical design, four number of OPNLM pixels are placed in (2x2) matrix form for PCM (type-1) and sixteen and sixty-four numbers of OPNLM pixels are placed in (4 x4) and (8x8) matrixes form for PCM (type-2) and PCM (type-3) respectively. The operation of a single OPNLM with setup for producing phase-conjugated beam is described as shown in figure 4. In the optical phase conjugation mechanism a beam can be created from another beam with equal frequency but opposite in phase.

Having same frequency one forward and one backward beams, which are known as Read Beam, are distinguishable by the different propagation and polarization directions and they are interacting in nonlinear medium, that has at least a cubic type of non-linearity. A conjugate beam is generated and reflected when the third probe beam having the same frequency is incident at a specific angle, provided the states of polarization of three interacting beam is identical, other than no such reflected beam is received. This property of the OPNLM can be used as an optical switch [29-35]. If the electric field vectors E_f, E_b and E_p of the forward, the backward and the probe beam respectively are combined in a cubic nonlinear medium at a point, the total field in the non-linear medium is, $\mathbf{E(t)} \propto \frac{1}{2}\left(\mathbf{E_f}+\mathbf{E_b}+\mathbf{E_p}+\mathbf{E_p^*}\right)^3$. Naturally the pump beam has high power than the probe beam. The induced cubic polarization creates a triple product of the conjugated input beam ($\mathbf{E_p^*}$) with the other two input beams E_f and E_b. As a result the desired beam ($\mathbf{E_p^*}$) in which the energy is transferred from probe beam has a multiplicative gain term. The above optical phase conjugation mechanism is used to keep the nonlinear material as an optical switch. When 1 and 2 Read Beams of laser incident from two opposite side of the OPNLM, an another input probe beam falls from a horizontally polarized light source, after partially reflected from a beam splitter (BS) to the OPNLM at the point of intersection of the two read beams. Then this another incident beam reflects back from that point along the same path to release the output beam. No output beam will be produced if either read beam 1 or read beam 2 is absent or both of them are absent and this switch will succeed if the two read beams are coherent in nature and same state of polarization [36].

IV. WALSH CODE GENERATION USING OPTICAL NONLINEAR MATERIAL

A. Walsh-Hadamard Code

The Walsh-Hadamard code is a linear code which maps binary strings of length n to binary codeword of length 2^n and these codes are mutually orthogonal. Walsh-Hadamard code creates orthogonal spreading codes for multicarrier CDMA system. Under perfect synchronization the orthogonal codes avoid Multiple Access Interference. These functions are governed by mapping codeword rows of a special square matrix known as Hadamard matrix [37]. So, Walsh code of N length can offer N number of codes which can assist maximum N number of CDMA users, and it can be produced by a standard repetitive procedure:

The Walsh-Hadamard Code are created in a set of $N=2^n$ codes with length $N=2^n$. The generating algorithm is very simple: $H_{N/2}=\begin{bmatrix} H_{N/2} & H_{N/2} \\ H_{N/2} & -H_{N/2} \end{bmatrix}$; with H_0 = [1]. The rows (or columns) of the matrix H_N are the Walsh-Hadamard Codes.

$$H_2 = \begin{bmatrix} 1 & 1 \\ 1 & -1 \end{bmatrix} \quad ; \quad -H_2 = \begin{bmatrix} -1 & -1 \\ -1 & 1 \end{bmatrix} \quad ; \quad H_4 = \begin{bmatrix} 1 & 1 & 1 & 1 \\ 1 & -1 & 1 & -1 \\ 1 & 1 & -1 & -1 \\ 1 & -1 & -1 & 1 \end{bmatrix};$$

$$H_8 = \begin{bmatrix} 1 & 1 & 1 & 1 & 1 & 1 & 1 & 1 \\ 1 & -1 & 1 & -1 & 1 & -1 & 1 & -1 \\ 1 & 1 & -1 & -1 & 1 & 1 & -1 & -1 \\ 1 & -1 & -1 & 1 & 1 & -1 & 1 & 1 \\ 1 & 1 & 1 & 1 & -1 & -1 & -1 & -1 \\ 1 & -1 & 1 & -1 & -1 & 1 & -1 & 1 \\ 1 & 1 & -1 & -1 & -1 & -1 & 1 & 1 \\ 1 & -1 & -1 & 1 & -1 & 1 & 1 & -1 \end{bmatrix}$$

In each above case the first row of the matrix consist entirely of 1s and each of the other rows contains N/2 -1s and N/2 1s. Row N/2 starts with N/2 1s ends N/2 -1s. The distance (number of different elements) between any pair of rows is exactly N/2. For H_8 the distance between any two rows is 4, so that the Hamming distance of the Hadamard code is 4. The Walsh-Hadamard code can be employed as a block code in channel encoder; each sequence of n bits identifies one row of the matrix (there are $N=2^n$ possible rows). All rows are mutually orthogonal:

$$\sum_{k=0}^{N-1} h_{ik} . h_{jk} = 0 \quad \text{for all rows i and j.}$$

B. Walsh-Hadamard (2x2) code generator using Composite (2x2) block and OPNLM matrix (2x2) block

The all-optical circuit for different logical operation of Walsh-Hadamard is displayed in the figure 5. A lights from two input coherent light sources A and B fall on IB-1 and IB-2, respectively. The orientation of IB-2 gets 90° anticlockwise shift with respect to IB-1 as shown in the Fig. 5. At first input beams enter the TOAD and after passing through the TOAD, beams are permitted to incident on IB 2x2 matrixes. The emerging horizontally polarized (•) beams from IB fall on OPNLM 2x2 matrix as shown in figure 5.

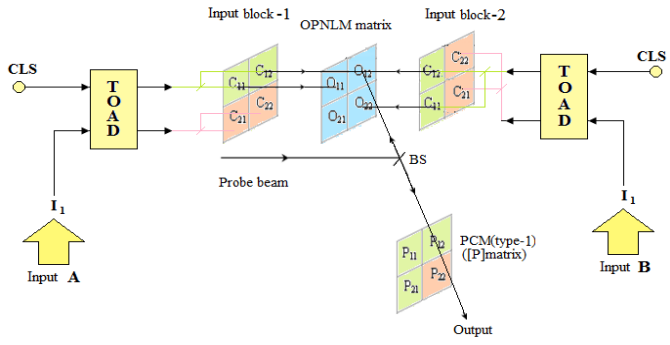

Fig.5. Setup for two input all optical logical operation of (2x2) Walsh-Hadamard Code

(a) If A=1 and B=1, i.e. horizontally polarized light; then horizontally polarized light (•) is come out from C_{11}, C_{12} pixels of both IB-1 and IB-2 blocks.
(b) If A=0 and B=0, vertically polarized light; then horizontally polarized light is come out from C_{21}, and C_{22} pixels of both IB-1 and IB-2 blocks.

Let us consider the case (i) A=1 and B=0. When A=1, O_{11}, and O_{12} pixels of OPNLM matrix receive horizontally polarized light (•) from IB-1 block in figure 5. At the same time, when B=0, O_{12}, and O_{22} pixels of the OPNLM matrix receive horizontally polarized light from IB-2 in figure 5. According to the switching mechanism of the OPNLM explained above in figure 4, that probe beam which is horizontally polarized light will be reflected only from O_{12} pixel of OPNLM matrix as shown in the figure 5.

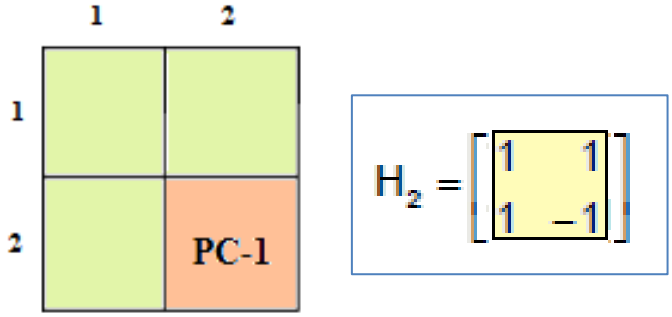

(a) (b)

Fig 6: (a) Front view of PCM (type-1) or [P] matrix plane for different states, (b) Hadamard (2x2) matrix

And case (ii) A=0 and B=1. When A=0, O_{21}, and O_{22} pixels of OPNLM matrix get horizontally polarized light (•) from IB-1 block. Again for B=1, O_{11}, and O_{21} pixels of the OPNLM matrix get horizontally polarized light (•) from IB-2 blocks. According to the switching mechanism of the OPNLM explained, the probe beam which is horizontally polarized light will be reflected only from O_{21} pixel of OPNLM matrix (not in figure 5). In this figure actually (2x2) = 4 probe beams are made incident on four separately distributed cells on OPNLM by four BSs (only one is shown in the figure 5). Probe beam is reflected from OPNLM matrix and it is allowed to pass through a PCM (type-1) matrix block. Light which comes out from PCM (type-1) is considered as the output of logical operation. For different logical operation, different PCMs are employed. The PCM (type-1) is displayed in the figure 6.

Table 5 Truth table of PCM (type-1) for Walsh code

A / B	1	0
1	1	1
0	1	-1

(1) If, A=1, B=1, the probe beam of horizontally polarized light (•) is reflected from O_{11} of OPNLM matrix and falls on P_{11} pixel on PCM (type-1) matrix. As no polarizer converter is present on P_{11} pixel of PCM (type-1) (figure 6), so horizontally polarized light (•) is come out from PCM (type-1) as output whose logic level is taken as 1. This indicates that A=1, B=1, output = 1 are satisfied as in table 5.

(2) As interpreted above if, A=1, B=0, the probe beam of horizontally polarized light (•) is reflected from O_{12} only and falls on P_{12} pixel of PCM (type-1). As no polarizer converter is present on P_{12} pixel of PCM (type-1) (figure 6), so horizontally polarized light (•) is come out from PCM (type-1) as output whose logic level is taken as 1. This indicates that A=1, B=0, output = 1 are satisfied as in table 5.

(3) If, A=0, B=1, the probe beam of horizontally polarized light (•) is reflected from O_{21} of OPNLM matrix and falls on P_{21} pixel on PCM (type-1) matrix. As no polarizer converter is present on P_{21} pixel of PCM (type-1) (figure 6), so horizontally polarized light (•) is come out from PCM (type-1) as output whose logic level is taken as 1. This indicates that A=0, B=1, output = 1 are satisfied as in table 5.

(4) If, A=0, B=0, the probe beam of horizontally polarized light (•) is reflected from O_{22} of OPNLM matrix and falls on P_{22} pixel on PCM (type-1) matrix. Then PC-1 converts horizontally polarized light (•) to plane polarized light at 45^0 ( ). Hence A=0, B=0 and output = -1 are satisfied as in table 5.

C. Walsh-Hadamard (4x4) code generator using Composite (4x4) block and OPNLM matrix (4x4) block

(1) If, A=1, B=1, the probe beam of horizontally polarized light (•) is reflected from O_{11} of OPNLM matrix and fall on P_{11} pixel on PCM (type-1) matrix in figure 8. Then PC-1 on P_{11} converts horizontally polarized light (•) to plane polarized light at 45^0 ( ). So, plane polarized light at 45^0 ( ) is come out from PCM (type-2) as output whose logic level is taken as -1. This indicates that A=1, B=1, output = -1 are satisfied as in table 6.

(2) As interpreted above if, A=1, B=0, the probe beam of horizontally polarized light (•) is reflected from O_{12} only and falls on P_{12} pixel of PCM (type-2) in figure 8. Then PC-1 on P_{12} converts horizontally polarized light (•) to plane polarized light at 45^0 ( ). So, plane polarized light at 45^0 ( ) is come out from PCM (type-2) as output whose logic level is taken as -1. This indicates that A=1, B=0, output = -1 are satisfied as in table 6.

(3) If, A=0, B=1, the probe beam of horizontally polarized light (•) is reflected from O_{21} of OPNLM matrix and fall on P_{21} pixel on PCM (type-2) matrix. A polarizer converter PC-1 is present on P_{21} pixel of PCM (type-2) in figure 8, so horizontally polarized light (•) is converted to plane polarized light at 45^0 ( ). Plane polarized light at 45^0 ( ) is come out from PCM (type-2) as output whose logic level is taken as -1. This indicates that A=0, B=1, output = -1 are satisfied as in table 6.

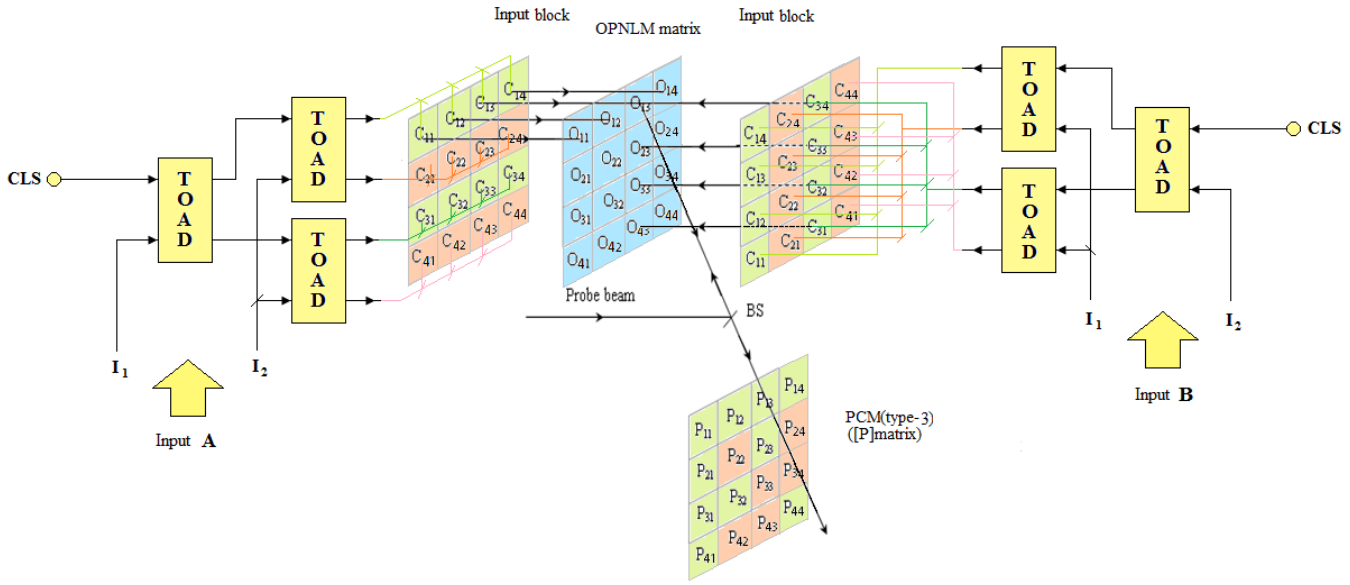

Fig.7. Setup for two input all optical logical operation of (4x4) Walsh-Hadamard Code

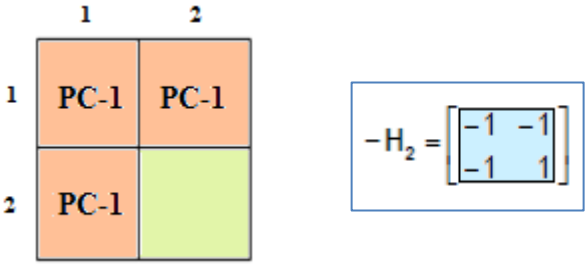

(a) (b)

Fig 8: (A) Front view of PCM (type-2) or [P] matrix plane for different states, (B) The inverse of Hadamard (2x2) matrix

Table 6 Truth table of PCM (type-2) for Walsh code

A / B	1	0
1	-1	-1
0	-1	1

(4) If, A=0, B=0, the probe beam is reflected from O_{22} of OPNLM matrix and fall on P_{22} pixel on PCM (type-2) matrix. As no polarizer converter is present on P_{22} pixel of PCM (type-2) in figure 8, so horizontally polarized light (⬮) is come out from PCM (type-2) as output whose logic level is taken as 1. This indicates that A=0, B=0, output = 1 are satisfied as in table 6.

PCM (type-3) matrix (4x4) blocks for Hadamard (4x4) matrix (H_4) of Walsh-Hadamard (4x4) Code Generation using PCM (type-1) and (type-2) matrix (2x2) blocks

It needs three PCM (type-1) and one PCM (type-2) to form PCM (type-3). PCM (type-1) and (type-2) matrix blocks arrangement in PCM (type-3) matrix blocks for Walsh-Hadamard Code Generation is shown in figure 9. And its operation is same as Walsh-Hadamard code generator using Composite block (2x2) and OPNLM matrix (2x2) block.

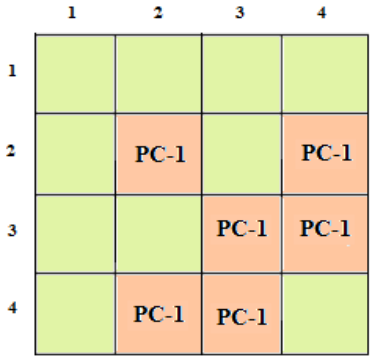

(a)

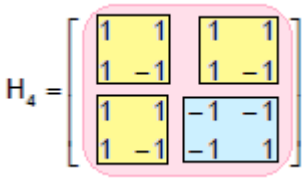

(b)

Fig.9. (a) Front view of PCM (type-3) or [P] matrix plane for different states, (b) Hadamard (4x4) matrix

The all-optical circuit for different logical operation as shown in the figure 7 is same as explained in the figure 5 and satisfies table-7.

Table-7: Truth table of PCM (type-3) for Walsh code using fig. 7

A / B	11	10	01	00
11	1	1	1	1
10	1	-1	1	-1
01	1	1	-1	-1
00	1	-1	-1	1

D. Walsh-Hadamard (8x8) code generator using Composite (8x8) block and OPNLM matrix (8x8) block

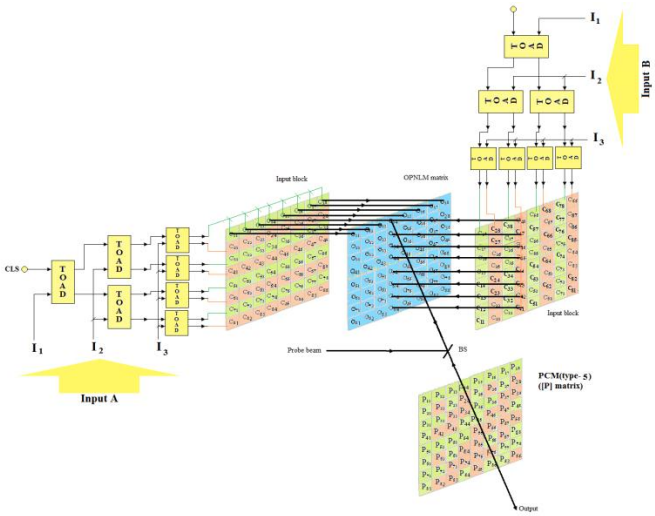

Fig.10. Setup for two input all optical logical operation of (8x8) Walsh-Hadamard Code

The all-optical circuit for different logical operation as shown in the figure 10 is same as explained in the figure 5.

1. PCM (type-4) matrix (4x4) blocks for the inverse of Hadamard (4x4) matrix (-H_4) of Walsh-Hadamard (8x8) Code Generation using PCM (type-1) and (type-2) matrix (2x2) blocks

It needs three PCM (type-2) and one PCM (type-1) to form PCM (type-4). PCM (type-1) and (type-2) matrix blocks arrangement in PCM (type-4) matrix blocks for Walsh-Hadamard Code Generation is shown in figure 11. And its operation is same as Walsh-Hadamard code generator using Composite block (2x2) and OPNLM matrix (2x2) block.

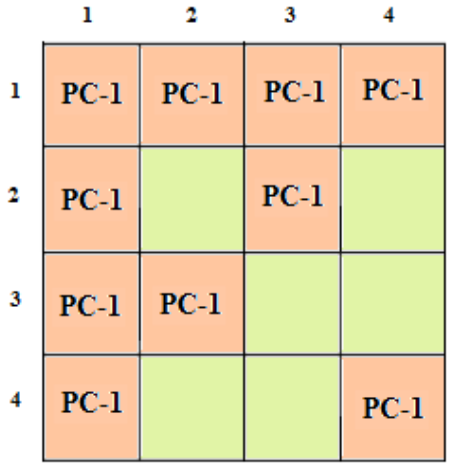

(a)

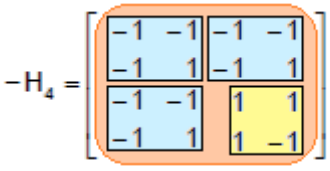

(b)

Fig.11. (a) PCM (type-1) and (type-2) matrix blocks arrangement in PCM (type-4) matrix blocks for Walsh-Hadamard Code Generation, (b) The inverse of Hadamard (4x4) matrix

2. PCM (type-5) matrix (8x8) blocks for Hadamard (8x8) matrix (H_8) of Walsh-Hadamard (8x8) Code Generation using PCM (type-3) and (type-4) matrix (4x4) blocks

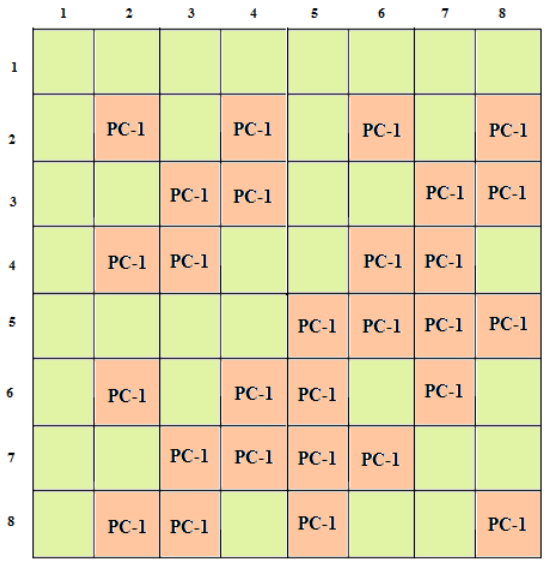

(a)

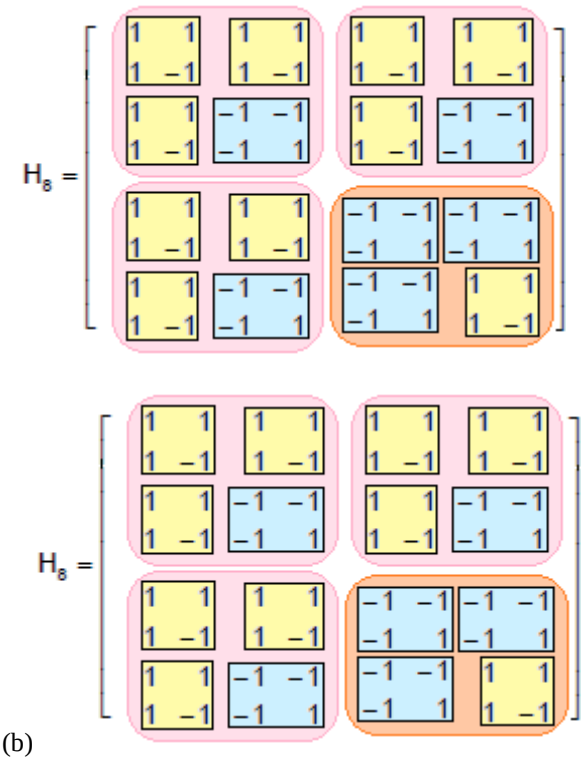

(b)

Fig.12. (a) PCM (type-3) and (type-4) matrix blocks arrangement in PCM (type-5) matrix block for Walsh-Hadamard Code Generation; (b) Hadamard (8x8) matrix

It needs three PCM (type-3) and one PCM (type-4) to form PCM (type-5). PCM (type-3) and (type-4) matrix blocks arrangement in PCM (type-5) matrix blocks for Walsh-Hadamard Code Generation is shown in figure 12. Its operation is same as Walsh-Hadamard code generator using Composite block (2x2) and OPNLM matrix (2x2) block and satisfies table 8.

Table-8: Truth table of PCM (type-5) for Walsh code using fig. 10

A / B	111	110	101	100	011	010	001	000
111	1	1	1	1	1	1	1	1
110	1	-1	1	-1	1	-1	1	-1
101	1	1	-1	-1	1	1	-1	-1
100	1	-1	-1	1	1	-1	-1	1
011	1	1	1	1	-1	-1	-1	-1
010	1	-1	1	-1	-1	1	-1	1
001	1	1	-1	-1	-1	-1	1	1
000	1	-1	-1	1	-1	1	1	-1

V. SIMULATION AND RESULTS

To experimentally achieve the result of the proposed scheme, some design parameters have to be assumed because the above discussions are based on simple model. As for example they are predetermined values of the intensities, polarization properties of fiber, wavelength of laser light for control and incoming signals, intensity losses due to beam splitters/fiber couplers, introduction of filter, etc. For practical implementation of all-optical circuit, the picoseconds Nd: YAG laser can be used as read beam and probe beam. Photo refractive BaTiO3 or some other nonlinear materials can be exploited to generate OPNLM matrix block. The system mentioned above may give picoseconds response time in connection to its speed of operations. Intensity losses due to couplers in interconnecting stage may not create such trouble in producing the desired optical bits at the output due to the whole system is digital one and the output depends only on the presence or absence of light signal.

The output logical states of every logical circuit can be measured by stokes vector [S] measurement. Stokes vector can be determined from the measurement of six intensities ($I_{i,}$

$_j$) in the photo detector (PD) by use of a linear analyzer (LA) followed by a quarter wave plate (λ/4 plate), which is shown in the figure 13. The formula for computing stokes vector is:

$$[S] = \begin{bmatrix} S_0 \\ S_1 \\ S_2 \\ S_3 \end{bmatrix} = \sqrt{\frac{\mu_0}{\varepsilon_0}} \begin{bmatrix} I_{(0,0^\circ)} + I_{(0,90^\circ)} \\ I_{(0,0^\circ)} - I_{(0,90^\circ)} \\ I_{(0,45^\circ)} - I_{(0,135^\circ)} \\ I_{\left(\frac{\lambda}{4},45^\circ\right)} - I_{\left(\frac{\lambda}{4},135^\circ\right)} \end{bmatrix}$$

Where first subscript ('*i*') index lack or presence of $\lambda/4$ plate and the second ('*j*') gives the azimuth of the analyzer. The μ_0 and ε_0 are free space permeability and permittivity. Degree of polarization (DOP) is also computed by the equation:

$$\text{DOP} = \frac{\sqrt{S_1^2 + S_2^2 + S_3^2}}{S_0}$$

The value of DOP can be plotted in Poincaŕe sphere in point 'P' and we determine that, for vertically (↕) and horizontally (•) polarized light OP=DOP=1 and lies on the equator of the Poincaŕe sphere (at point *y* and *x* respectively).

In high speed data communication (50 GB/s or TB/s) random change of polarization in a short time can produce power fluctuation at the output. So polarization dependent loss (PDL) degrades the optical signal to noise ratio (OSNR) and also degrades the extinction ratio. PDL of 3 dB could cause 1 dB power penalty [35]. Optical depolarizers can be employed to reduce the polarization-induced noise in optical sensing and measurement systems [34]. Optical depolarizers can be inserted to reduce the polarization-induced noise in optical sensing and measurement systems. Again random birefringence in optical fibers induces an unpredictable rotation of the sate of polarization (SOP); this can be adjusted by using polarization controller and PM fiber. Intrinsic cross talk between two polarization states, imperfection of polarized tracking after transmission link etc may cause polarization mode dispersion (PMD). This may cause the delay among the different states of polarization. The effects of PMD are expected to be similar to those of other approaches that have been studied in the literature.

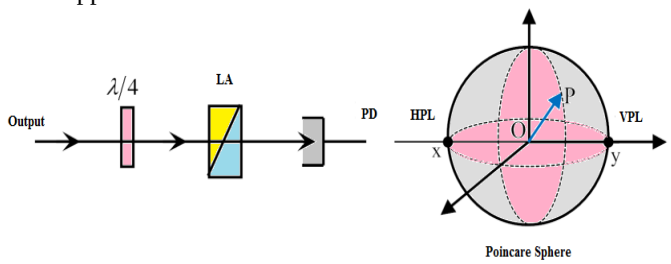

Fig.13 Stokes vector [S] measurement

Optical amplifiers degrade the signal-to-noise ratio (SNR) of the amplified signal because of spontaneous emission added to the signal during its amplification (ASE). The OSNR-errors arise in this process. For polarized signal PHB will cause ASE polarization orthogonal to the signal polarization. Bruyere et al have reported that the DOP of ASE could exceed 70% in transoceanic links with low PMD [38]. Of course, the most of ASE light does not traverse the entire light path, and then OSNR-errors become less as < 0.6 dB.

Polarization related problem discussed above would occur inside the considered circuit. The said problem will not occur in optical communications system once the signal comes out the output. State of polarization may be changed if it is passed through bi-refringent crystals or optically active substances. The significant advantage of this proposed scheme is that the schemes are all-optical in nature and can be easily and successfully be extended for higher order. This scheme is easily practicable as the components of our design are technically highly developed and vastly used in optical communication.

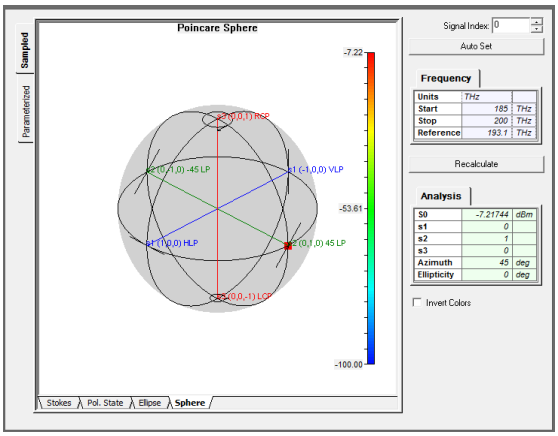

(a)

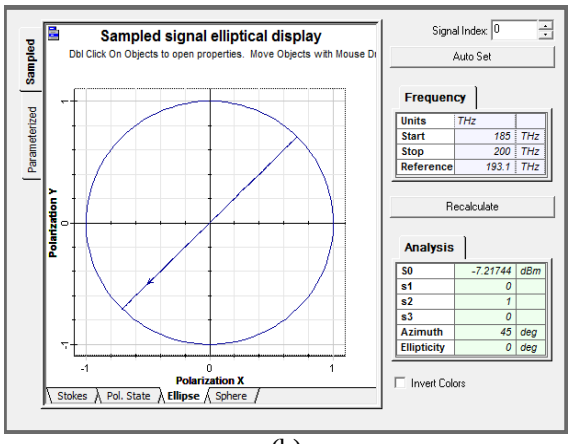

(b)

Fig. 14 (a) Simulation of Poincaŕe sphere by Optisystem 7.0, (b) Simulation of Polarization state of light signal by Optisystem 7.0

A. Mathematical simulation by Matlab-9 for H_2 (2x2) matrix

The mathematical simulation is done by Matlab-9 for H_2 (2x2) matrix as given below.

(i) Hadamard H_2 (2x2) matrix

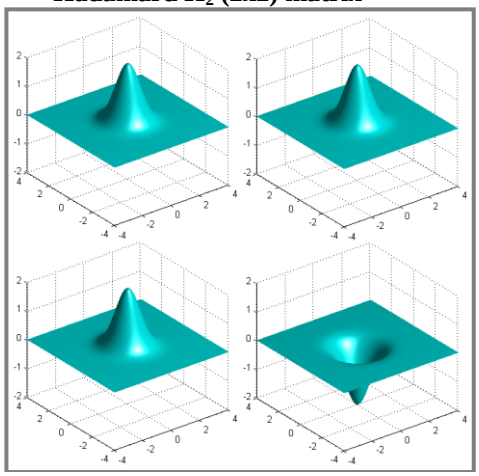

Fig.15. Hadamard H_2 (2x2) matrix

(ii) The inverse of Hadamard $-H_2$ (2x2) matrix

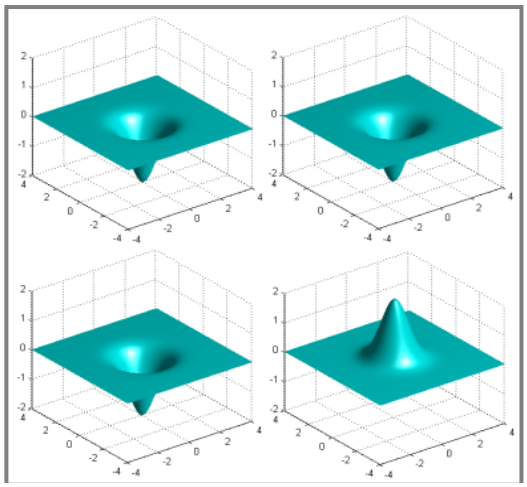

Fig. 16.Hadamard $-H_2$ (2x2) matrix

B. Mathematical simulation by Matlab-9 for H_4 (4x4) matrix

The mathematical simulation is done by Matlab-9 for H_4 (4x4) matrix as given below.

(i) Hadamard H_4 (4x4) matrix

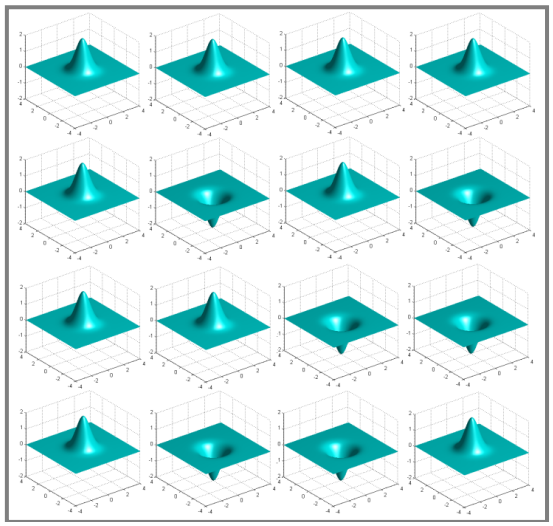

Fig.17. Hadamard (4x4) matrix, H_4

(ii) The inverse of Hadamard $-H_4$ (4x4) matrix

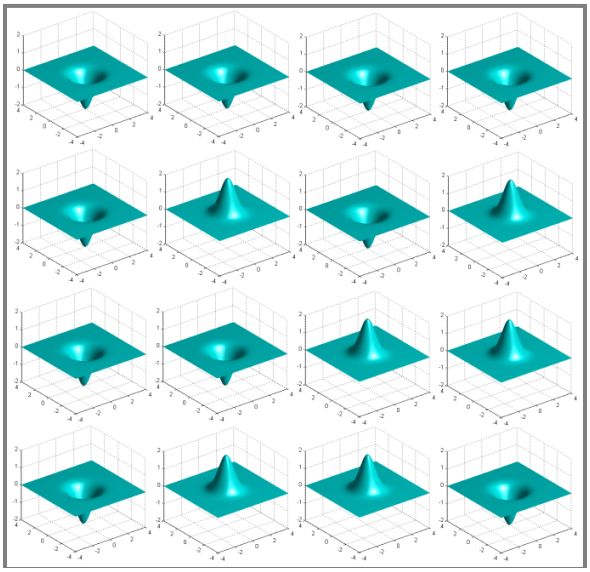

Fig.18. Hadamard $-H_4$ (4x4) matrix

C. Mathematical simulation by Matlab-9 for H_8 (8x8) matrix

The mathematical simulation is done by Matlab-9 for H_8 (8x8) matrix as given below.

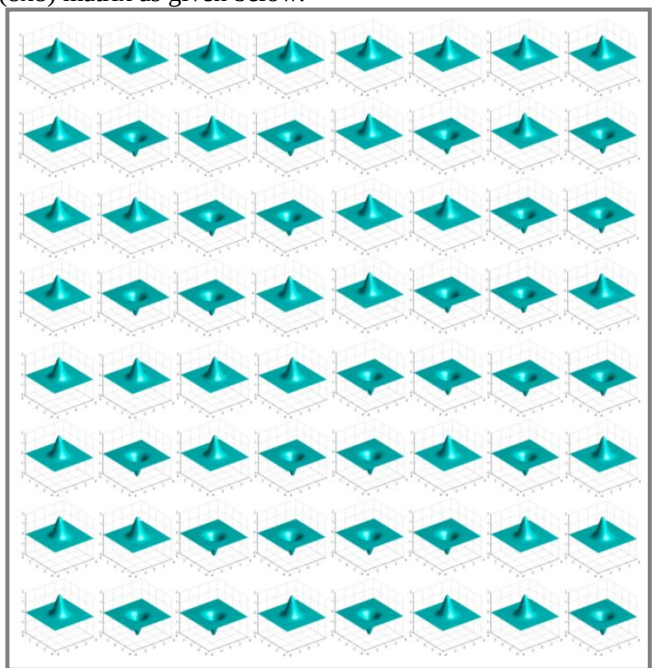

Fig.19. Hadamard H_8 (8x8) matrix

VI. Conclusion

In a CDMA system availability of more number of codes, minimum magnitude of cross correlation, impulsive peak auto correlation and bit error rate (BER) performance plays a major role. So Code designer have to generate spreading code such that it support more number of user, good auto-correlation property, good BER performance with better cross-correlation property which eliminate undesirable effect by reducing the chance of false synchronization. This paper present one algorithm to generate "a novel orthogonal minimum correlation spreading code" which offer a large number of codes in comparison to other existing code like Walsh code and OKasami code with better auto and cross correlation property. Hence we concluded that purposed all-optical Walsh-Hadamard code outperform other existing code and give one optimum solution for future CDMA communication system. CDMA technology is a fast growing technology in the field of Wireless Communication. The ultimate aim of service providers is to accommodate the maximum number of users in the available bandwidth. CDMA technology is identified by its spreading capability through the spreading codes for multiple accessing various users information. The design of an all-optical Walsh-Hadamard code generator has been theoretically discussed and established. The proposed scheme depends on optical non-linear material for Walsh code generation. The code building block for these modules is the OPNLM. The design of Walsh-Hadamard code generator is very promising regarding the issue of versatility and compactness. The design can be applied and extended for diverse application for Walsh-Hadamard codes are needed.

REFERENCES

[1] D. Woods & T.J. Naughton, Photonic neural networks. Nature Physics, 8, doi: 10.1038/nphys2283, 257 (2012).

[2] B. M. Popovic, "Spreading sequences for multicarrier CDMA systems," IEEE Trans. Communication., vol. 47, no. 5, pp. 918 (1999).

[3] H.J. Caulfield, S. Dolev & W.M.J. Green, Appl. Opt. A, 48 (Optical High-Performance Computing feature issue), http://dx.doi.org/10.1364/AO.48.0OHPC1 (2009).

[4] S. P. Maity, M. Mukherrjee, "On Optimization of CI/MC-CDMA System", In: 20th IEEE Personal, Indoor and Mobile Radio Comm. Symp., Japan, pp. 3203 (2009).

[5] T. Reed, G. Mashanovich, F.Y. Gardes & D.J. Thomson, Silicon optical modulators. Nature Photonics, 4, doi:10.1038/nphoton.2010.179, 518 (2010).

[6] G. W. Wornell, "Spread-signature CDMA: Efficient multi-user comm-unication in the presence of fading," IEEE Trans. Inform. Theory, vol. 41, no. 5, pp. 1418 (1995).

[7] H.J. Caulfield & S. Dolev, Why future supercomputing requires optics. Nature Photonics, 4, doi:10.1038/nphoton.2010.94, 262 (2010)

[8] C. Taraphdar, T. Chattopadhyay & J.N. Roy, Designing of Polarization encoded all-optical ternary multiplexer and Demultiplexer. Recent Patents on Signal Processing, 1(2), 143, doi:10.2174/1877612411101020143 (2011).

[9] J. Li, L. Li, L. Jin and C. Li, "All-optical switch and limiter based on nonlinear polarization in Mach-Zehnder interferometer coupled with a polarization maintaining fiberring resonator," Optics Communication, vol.260, pp.318 (2006).

[10] T. Chattopadhyay, J.N. Roy & A.K. Chakraborty, Polarization encoded alloptical quaternary R-S flip-flop using binary latch. Optics Communications, 282, 1287-1293, DOI:10.1016/j.optcom.2008.12.022 (2009).

[11] C. Ji, R. G. Broeke, Y. Du, J. Cao, N. Chubun, P. Bjeletich, F. Olsson, S. Lourdudoss, R. Welty, C. Reinhardt, P. L. Stephan, and S. J. B. Yoo, "Monolithically integrated InP based photonic chip development for O-CDMA systems," IEEE J. Select. Topics Quantum Electron, vol. 11, pp. pp66 (2005).

[12] S. Liu, C. Li, J. Wu and Y. Liu, "Optoelectronic multiple-valued logic implementation," Optics Letters, vol.14(14), pp.713 (1989).

[13] G. Eichmann, Y. Li and R. R. Alfano, "Optical binary coded ternary arithmetic and logic," Applied Optics, vol.25(18), pp.3113 (1986).

[14] G. K. Maity, S. P. Maity and J. N. Roy, "All-Optical Manchester Code Generator using TOAD-based D Flip-Flop," ICDCS (2012).

[15] G.K. Maity & S.P. Maity, Realization of Orthogonal Codes in Optical Information Processing, IEEE International Conference on Emerging Applications of Information Technology, 978-1-4673-1827, 307 (2012).

[16] G. K. Maity, S. P. Maity and J. N. Roy, "TOAD-based All-Optical Gold Code Generator," ICDCS (2012) .

[17] G. Shvets, Optical polarsizer/isolator based on a rectangular waveguide with helical grooves, arxiv:physics/0606206v1 [physics.Optics], 1 (2006).

[18] J. P. Sokoloff, P. R. Prucnal, I. Glesk, M. Kane, A terahertz optical asymmetric demultiplexer (TOAD), IEEE Photon. Techno. Lett. 5 (7), 787-789, 1993.

[19] J. P. Sokoloff, I. Glesk, P. R. Prucnal, R. K. Boneck, Performance of a 50 Gbit/s Optical Time Domain Multiplexed System Using a Terahertz Optical Asymmetric Demultiplexer, IEEE Photon. Techno. Lett.6 (1), 98-100, 1994.

[20] Y.K.Huang, I.Glesk, R.Shankar, P.R.Prucnal, Simultaneous all-optical 3R regeneration scheme with improved scalability using TOAD, Optics Express, 14(22), 10339-10344, 2006.

[21] Z.Y. Shen and L. L. Wu, Reconfigurable optical logic unit with a terahertz optical asymmetric demultiplexer and electro-optic switches, Appl. Opt. 47(21), 3737-3742, 2008.

[22] B.C. Wang, V. Baby, W. Tong, L. Xu, M. Friedman, R.J. Runser, I. Glesk, P. R. Pruncnal, A novel fast optical switch based on two cascaded Terahertz Asymmetric Demultiplexers(TOAD), Optics Express 10(1), 15-23, 2002.

[23] Y. J. Jung, S. Lee, N. Park, All-optical 4-bit gray code to binary coded decimal converter, Optical Components and Materials, Proceedings of the SPIE, Volume 6890, 68900S, 2008.

[24] J.N.Roy, D.K.Gayen, Integrated all-optical logic and arithmetic operations with the help of TOAD based interferometer device – alternative approach, Appl. Opt. 46(22), 5304-5310, 2007.

[25] J. N. Roy, G. K. Maity, D. Gayen, T. Chattopadhyay, Terahertz Optical Asymmetric Demultiplexer based tree-net architecture for all-optical conversion scheme from binary to its other 2n radix based form, Chinese Optics Letter 6(7), 536-540, 2008.

[26] R. Menzel, Photonics Linear and Nonlinear Interactions of Laser Light and Matter (Springer-Verleg, Barlin, Heidelberg, Chap. 4 (2006).

[27] G.S. He, Prog. Quantum Electron. 26 (3) (2002) 131.

[28] A. Yariv, D.M. Pepper, Opt. Lett. 1 (1) (1977) 16.

[29] A.W. Lohmann, Polarization and optical logic, Applied Optics, 25, 1594 (1988).

[30] J.M. Tang, & K.A. Shore, Strong picosecond optical pulse propagating in semiconductor optical amplifiers at transparency. IEEE Journal of Quantum Electronics, 34(7), 1263-1269, doi: 10.1109/3.687871 (1998).

[31] A.W. Domanski, Polarization degree fading during propagation of partially coherent light through retarders. Opto-Electronics Review, 7th International Workshop on Nonlinear Optics applications, 13(2), 171 (2005).

[32] S.L. Hurst, Multiple-Valued Logic-Its Status and its Future, IEEE Transactions on computers, C-33(12), 1160, Doi:10.1109/TC.1984.1676392 (1984).

[33] F. Bruyere & O. Andouin, Penalties in long-haul optical amplifiers systems due to polarization dependent loss and gain. IEEE Photonics Tech. Letters, 6(5), 654, doi: 10.1109/68.285570 (1994).

[34] L.E. Nelson, T.N. Nielson & H. Kogelnik, Observation of PMD-induced coherent crosstalk in polarization-multiplexed transmission. IEEE photonics tech. letter, 13(7), 738, DOI:10.1109/68.930432 (2001).

[35] A. Mecozzi & M. Shtaif, 'The statistics of polarization dependent loss in optical communication systems'. IEEE photonics tech. letter, 14(3), 313, DOI: 10.1109/68.986797 (2002).

[36] T. Chattopadhyay, G. K. Maity, J. N. Roy, "Designing of all-optical tri-state logic system with the help of optical nonlinear material," Journal of Nonlinear Optical Physics and Materials, vol.17, No. 3, 315 (2008).

[37] J.L. Walsh, A closed set of normal orthogonal functions. American Journal of Mathematics, 45(1), 5 (1923).

[38] F. Bruyere & O. Andouin, O 'Penalties in long-haul optical amplifiers systems due to polarization dependent loss and gain'. IEEE Photonics Tech. Letters, 6(5), 654, doi: 10.1109/68.285570 (1994).

Authors Profile

Ashis Kumar Mandal was born in Howrah, West Bengal on 15th March, 1980. He received BSc (Hons. In Physics) degree from Calcutta University, MSc (Physics) from Madurai Kamaraj University and Ph. D. from Jadavpur University, Kolkata. He is presently working as an Assistant Teacher in Chakur Haris Seminary High School. With nearly 12 years of teaching experience he passed CSIR-UGC NET-2012 (LS, Rank-70) in India. He is interested in digital electronics, optical information processing in communication system and organic solar cell.

